Sigma Journal of Engineering and Natural Sciences
Web page info: https://sigma.yildiz.edu.tr
DOI: 10.14744/sigma.2025.1938

Research Article

Simulation of engine oil driven second grade ternary hybrid nanofluid flow subject to thomson and troian slip velocity addressing the thermo-convection effect

Tusar Kanti DAS[1,*], Mintu SAUD[1], Nayanto HAJONG[1], Bidyut KALITA[1]

[1]*Department of Mathematics, Dudhnoi College, Dudhnoi, Assam, 783124, India*

ARTICLE INFO

Article history
Received: 12 June 2024
Revised: 03 August 2024
Accepted: 06 November 2024

Keywords:
Critical Shear Rate; Exponential Heat Source; Second-Grade Ternary Hybrid Nanofluid; Suction Effect; Thermo-Convection Effect; Thomson; Troian Slip Velocity

ABSTRACT

The furnished article primely focuses on the second-grade ternary hybrid flow and thermal characteristics triggered by vertical stretching sheets, featured with buoyant and thermo-convection effect subjects to Thomson and Troian velocity slip at the boundary. The ternary hybrid Nanofluid is composed of engine oil blended with three distinct nanocomposites: Ag, Cu, and graphene. Furthermore, the thermal boundary layer equation addresses the nonlinear exponential heat source and the thermo-convection effect. The aforementioned assumption leads to a schematic model framed with coupled partial differential equations revamped into an array of coupled ordinary differential equations via some relevant similarity variable, which are numerically solved by the bvp4c method. The novel contribution embraces the impact of Thomson and troian slip velocity, thermo-convection parameter, and exponential power law index alongside the second-grade fluid factor and suction parameter over the flow and thermal trajectory outline. It is noteworthy that the augmented variation in Thomson and Troian slip velocity and suction parameters diminished the flow pattern, but the opposite trend is noted with the escalating parameters such as second-grade fluid factor and critical shear rate. Moreover, the thermal diffusion profile appears in an elevated pattern with increased Thomson and Troian slip velocity, exponential heat source, and power law index. Beyond these, the heat transfer rate in the vicinity of the wall promptly rises with the augmentation in the Second-grade fluid parameter, critical Shear rate, thermos convection parameter, suction parameter, and power law index. Researchers can build on these findings to explore new material combinations and refine theoretical fluid dynamics and thermal management models.

Cite this article as: Das TK, Saud M, Hajong N, Kalita B. Simulation of engine oil driven second grade ternary hybrid nanofluid flow subject to thomson and troian slip velocity addressing the thermo-convection effect. Sigma J Eng Nat Sci 2025;43(6):2234–2247.

***Corresponding author.**
*E-mail address: tusarkantidas1995@gmail.com, dastusar95@dudhnoicollege.ac.in

This paper was recommended for publication in revised form by Editor-in-Chief Ahmet Selim Dalkilic

INTRODUCTION

Hybrid Nanofluid and its Application

Hybrid nanofluids stand as innovative pioneers in fluid dynamics as they are engineered by integrating various nanoparticulate species into the foundational composition of fluids. Additionally, after numerous studies conducted to determine the performance of these alternative fluids, they display enhanced thermal conductivity and heat preservation capabilities within various industrial sectors. The performance differences and improvements emanate from the interaction of the different types of nanoparticles, leading to a boosted thermal conductivity and optimal performance in heat transfer. The stability of these kinds of fluids can be acquired by escalating the individual dispersion of nanoparticulate, fending off the particle agglomeration. Furthermore, the better aspect ratio and the synergistic impacts of nanocomposite contribute to their comprehensive performance. Also, the boosted heat conductivity of nano-fluidics conveyed tangible convenience such as prompt energy control efficacy, brushing up the performance and structure, and optimizing expenses and costs. This makes them advantageous for supplication where efficient thermal dissipation and heat management are censorious, such as refrigeration structures for microchip technology, locomotive appliances, and heat exchangers. Ongoing research and development in this area aim to optimize Hybrid nanofluids› properties further to address specific needs in various industries, including energy production, electronics, and manufacturing.

Literature Review

Roy and Pop [1] inspected a second-grade hybrid nanofluid›s flow and heat conduction feature over a stretching sheet. Second-grade fluids demonstrate non-Newtonian behavior, distinguished by a nonlinear alliance between stress and strain rate. Hybrid nanofluids are a blending of unadventurous base fluids and nanoparticles, known for their improved thermal conductivity alongside heat conduction properties. By inquiring about advanced scientific mathematical flow modeling to assess the dynamics and the innovative mechanisms of heat transmission in processes that involve advanced engineering industrial utilization, such as cooling mechanisms and heat management over electronic devices, Nadeem et al. [2] conducted a computational breakdown of a second-grade fuzzy hybrid nanofluid flow across a stretching/shrinking surface.This inquiry has recourse to numerical simulation to characterize flow and thermal allocation, laying out visions for augmenting the transfer of thermal energy processes in implementation, for instance, solar collectors› thermal power storage systems. Jawad et al. [3] probed into the features of radiative second-grade hybrid nanofluid flow subjected to Lorentz force. By exploring the reciprocation between radiation, nanoscale particulates, and non-Newtonian flow features, the investigation grants consideration to phenomena pertinent to magnetic fluid actuators and drug-targeting structures. Roy and Ghosh [4] explored magneto-dynamic (MHD) free convection about second-grade hybrid Nanofluid across an adjustable thermos-flux surface. The concurrent study inquires how discrepancy in thermo-flux significantly exerts an impact on the heat transfer mechanism that involves convection, offering intuitions into designing coherent cooling devices, geothermal power extraction, and elevating thermal comfort in assembling and molding environments. Sakthi et al. [5] scrutinized the entropy generation of second-grade hybrid Nanofluid around a diverging passage, emphasizing the hyperthermia therapeutic facet that involves hauling up the temperature of intended tissues to persuade therapeutic effects, such as cancer treatment. Improvement of heat transfer efficiency in various engineering and biomedical applications. Zulqarnai et al. [6] examined the effect of entropy generation on exponentially permeable stretching/shrinking surfaces in second-order fuzzy hybrid nanofluids. Understanding and minimizing entropy generation is important to optimize the design and operation of thermal systems, energy conversion devices, and environmental management systems. Hosseinzadeh et al. [7] Investigated the second-order viscoelastic non-Newtonian nanofluid flow over a curved stretching surface in the appearance of MHD. Both viscous and elastic features which are present in viscoelastic fluid often found in biological fluids and polymer solutions. This reasearch explored the impact of magnetic flow behavior, providing perception into controlling fluid dynamics in abundant applications, such as medication administration, polymer manufacturing, and biomedical devices. Shah et al. [8] presented an alternative evaluation of the Cattaneo-Christov framework applied to magnetohydrodynamic second-grade nanofluid motion, incorporating with Soret and Dufour effects. The Cattaneo–Christov model extends Fourier›s law to account for finite thermal wave propagation velocities, while the Soret and Dufour effects expound mass and thermal diffusion in fluid flow, respectively. The study of heat and mass transport in magnetically influenced nanofluid systems, relevant to processes like energy conversion and material fabrication, necessitates an assessment of Soret and Dufour influences in MHD nanofluid motion. Abbas et al.[9] performed a numerical investigation of chemically reactive second-order nanofluid flow past an exponentially curved stretching surface. Chemical reactions within a fluid can significantly change its flow and heat transfer properties. The research provides intuition into the optimization of chemical processes such as nanoparticle synthesis, catalytic reactions, and biochemical engineering applications. Zaman et al. [10] computationally scrutinized an unsteady second-order bio-magnetic micropolar blood-based nanofluid flow with moving gyro taxis microorganisms. The research looked at the complex issues of biofluids, microbes, magnetic fields and nanocrystals. Understanding such phenomena is key in biomedical applications, such as biodegradation of compounds

and drug transport also in which regard to environment microbes in action within living systems. Gangadhar et al. [11] examined the effects of anomalous heat absorption and Arrhenius energy on the MHD flow of a generalized second order fluid over a nonlinear stretching surface, in the light of Cattaneo-Christov thermal absorption theory and thermal radiation. Arrhenius energy describes the temperature dependence of reaction rates in chemical kinetics, while anomalous thermal absorption delineates the uneven absorption of energy in a liquid. This research enhances comprehending of thermal transfer processes in intricate fluid flows relevant to environmental engineering, industrial processes and material synthesis. Farooq et al. [12] performed a computational study on convective thermal transfer in second-order MHD nanofluid flow across a stretching surface through a porous medium. In various engineering applications such as thermal exchangers, filtration and underground fluid flow, porous media are crucial. Understanding the interface between fields, nanofluids, and porous structures is important for optimizing thermal transfer and fluid flow in porous media-based systems. Rath and Nayak [13] investigated the higher-order MHD movement of a nanofluid over a deformable plate, considering the influences of activation energy along with thermophoresis and Brownian motion phenomena. A thin viscous effects in which a substance is held to a solid surface is what we term slip flow. Thermophoresis, Activation energy, and brownian motion play a vital role in particle transport and thermal transfer in nanofluidic flows in which we see also to include issues related to nanoparticle synthesis, nanofluidic heat exchangers, and microfluidic systems. Naveed Khan et al. [14] observed chemically reactive elements in the boundary layer flow of a second order nanofluid over an exponentially stretching surface. Stagnant point flows which are placed in a variety of engineering applications including heat transfer, combustion, and aerodynamics.In these flows comprehending chemical reactions is critical for optimising processes such as jet flow control in propulsion systems, combustion, and chemical vapor deposition.

Recent advancements in the study of second-grade hybrid nanofluids and fluid dynamics have been highlighted through numerous investigations focusing on the intricate behavior of diverse nanofluids under different conditions. Kezzar et al. [15] explored the impact of slip velocity and temperature jump on entropy generation in second-grade hybrid nanofluids within Jeffery-Hamel flow, shedding light on innovative approaches to heat management and fluid efficiency in complex flows. Reza-E-Rabbi et al. [16] performed a computational investigation to examine how radiative heat transfer influences nonlinear second-grade nanofluids in the presence of Arrhenius activation energy and sinusoidal magnetic forces, thereby advancing the understanding of complex nanofluid behaviors.Additionally, Haq and Ali [17] examined fractional hybrid nanofluids subjected to transverse magnetic fields, highlighting key aspects of Newtonian thermal behavior and the role of magnetic effects in governing heat transport. Finally,The MHD flow of second-grade fluids including shedding light on the combined effects of magnetic fields, thermal convection, nanoparticles with gyrotactic microorganisms across a heated convective sheet, and biological microbes on fluid behavior was investigated by Ahmed et al. [18]. These studies enhance our understanding of magnetic influences and thermal phenomena in complex fluid systems and nanofluid dynamics.

According to recent research on nanofluids emphasize their especial flow and thermal properties, importantly impacting thermal transfer processes across abundant applications. AKAJE et al. [19] investigate the heat and mass transfer dynamics in Casson nanofluids influenced by variable inclined magnetic fields, emphasizing how such conditions can optimize thermal performance. However, Li et al. [20] analyzed the behavior of ternary nanofluids over a stretching sheet, taking into account the velocity slip effects. El Hattab et al. [21] examined magnetohydrodynamic (MHD) natural convection within a square cavity utilizing carbon nanotube–water nanofluids, demonstrating how fin con y urations contribute to enhanced thermal dissipation. The investigation by Nath et al. [22] focused on MHD Casson hybrid nanofluid flow across porous cylindrical boundaries, revealing the complex interplay between structural hierarchy and magnetic influences [23-26]. In addition to the aforementioned research, some other explorer [27-29] put forward there handy contribution in the context of nanofluid.

The Novel Features and Applications of the Prescribed Model

This scientific survey emphasize that no prior research has presented a pioneering model that intricately combines an exponentially varying thermal source, the effects of thermo-convection and buoyancy on fluid flow across a stretching surface. A ternary hybrid nanofluid composed of silver (Ag), copper (Cu), and graphene which is known for exceptional heat properties are the main character of this model. This model examine synergetic effects of these three different nanoparticles by interacting them and supplying how they combine to impact thermal transfer and fluid dynamics. A large enhancement in displaying realistic fluid behavior is introduced by consideration of Thomson and Trion slip conditions at the boundary surface especially at the microscale where slip phenomena have a significant affect on performance. As per the author's concern, no prior investigation has been carried out combining this effect over the considered geometry. To computationally solve the designed problem, the bvp4c approach will be employed.

Furthermore, the present model has several applications that primely include enhanced thermal management. In high-tech applications such as thermal exchangers, electronic devices and high-performance cooling systems the model's detailed analysis can be directly applied to enhance heat management systems. Superior thermal dissipation

and energy efficiency can be obtained by improving the hybrid nanofluid composition. However, The perception from this model can help in the enhancement of manufacturing processes like polymer processing and thin-film deposition which involves in stretching surface. Stretching surfaces and hibrid nanofluids cobined to improve the process efficiency and product quality.

Infact, buoyancy effects models and the thermo-convection are essential for designing cooling systems in automotive and aerospace applications. Reliability and efficiency of aerospace and engines components are increased depending on enhanced cooling performance. The model›s exploration of exponentially varying heat sources provides valuable guidance for optimizing heat transfer and energy conversion processes for renewable energy technologies like solar thermal collectors.

The primary purpose of this investigation are:

- What insightful examination of thermal diffusion across stretching surface can be procured from the numerical simulation of second-grade ternary hybrid nanofluid?
- To discuss the consequences of suction velocity on the Nusselt number.
- How promptly does the thermo-convection factor affect the flow trajectory and thermal transmission?
- How does the Thomson and Troian slip velocity create an impact on the flow behavior and the characteristics of thermal transmission?
- Moreover, in what manner does the exponential heat source influence the simultaneous flow configuration within the framework of thermal transport?

In essence, this study analyzes the behavior of a ternary second-grade hybrid nanofluid in relation to heat dispersion over a stretching interface. Furthermore, the work examined the impact of suction velocity on the Nusselt number, examines the thermoconvection parameter's role in dictating both thermal distribution and flow dynamics, scrutinizes the influence of Thomson and Troian slip phenomena on thermal transport and momentum, and evaluates the modifications initiated by an exponential thermal source to the flow pattern and overall thermal transfer behavior.

MATHEMATICAL FORMULATION

The Crosser-Hamilton model (Abbas et al.[23]) based, A two-dimensional steady and incompressible second-grade ternary hybrid nanofluid flow is taken into account via a vertical stretching sheet. *Ag, Cu* and *Graphene* are the three nanocomposites used in the composition of ternary hybrid Nanofluid. The total volume fraction is kept below 15%. The high flexibility and resistance of graphene, the greater thermal conductivity of Cu, and the higher electric conductivity of Ag are the reasons behind the use of these nanoparticles in industrial and engineering applications that involve the heat transfer phenomena. The following are the underlying assumptions:

- The prescribed flow is assumed to be generated by the stretching surface.
- The velocity in the vicinity of the wall is prescribed as $u_w = bx$ as depicted in Figure 1.
- Furthermore, Thomson and Troian slip velocity is considered.
- An exponential heat source is considered, where n, indicates the power law index.
- The thermo-convection effect reflected by the term γ is also preferred in the concurrent model. Here, $\gamma = \frac{\partial T_\infty}{\partial y} + \frac{g}{c_p}$ is the vertical thermal convection parameter, which can

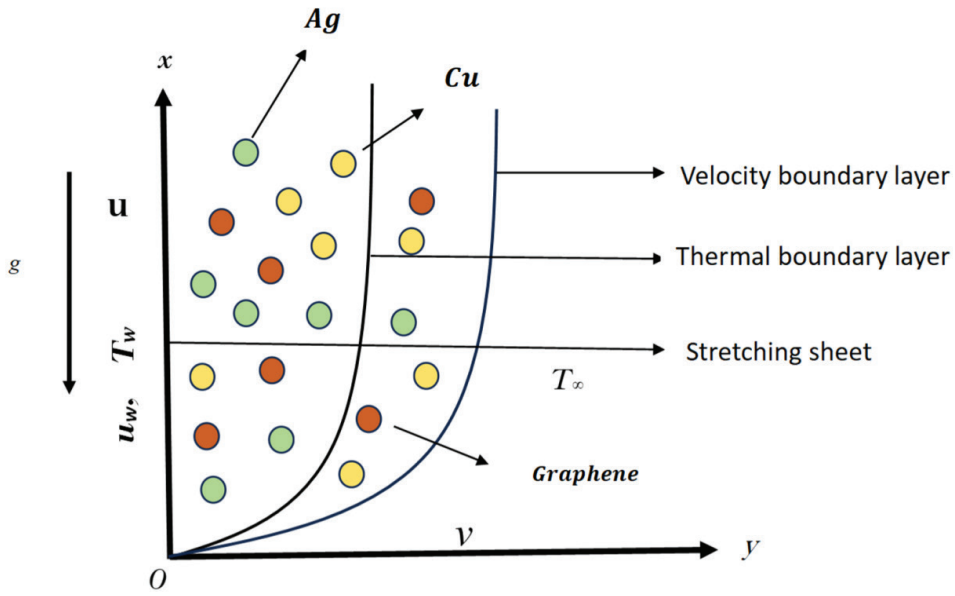

Figure 1. Physical flow diagram of the proposed model.

also be termed as a stratification parameter. Here, the term $\frac{g}{C_p}$, that indicates the rate of reversible work settled by the prescribed fluid is presumed to be negligible; thus, the role of the term $\frac{\partial T_\infty}{\partial y}$ is decisive.

- The Nanofluid chosen for the ongoing problem is composed of *Ag, Cu,* and graphene nanoparticles dispersed in ethylene glycol.
- The temperature at the vicinity of the surface, T_w is assumed to be greater than the ambient temperature, T_∞.

By addressing the aforementioned assumption, the mathematical model turns out to be the following form of governing equations. (Shah et al. [8], Li et. al. [20], Deka and Paul [24])

$$\frac{\partial u}{\partial x} + \frac{\partial v}{\partial y} = 0 \tag{1}$$

$$u\frac{\partial u}{\partial x} + v\frac{\partial u}{\partial y} = \frac{\mu_{THnf}}{\rho_{THnf}}\frac{\delta^2 u}{\delta y^2} + \frac{2\alpha_1}{\rho THnf}\frac{\delta u}{\delta y}\frac{\partial^2 u}{\partial x \partial y} - g\beta_T\,(T - T_\infty) \tag{2}$$

$$u\frac{\partial T}{\partial x} + v\frac{\partial T}{\partial y} = \frac{K_{THnf}}{(\rho C_p)_{THnf}}\frac{\partial^2 T}{\partial y^2} + \frac{Q}{(\rho C_p)_{THnf}}(T - T_\infty).e^{-ny}\sqrt{\frac{b}{v_f}} - \gamma u \tag{3}$$

The Boundary Constraints are (Li et. al.[20])

$$u = u_w + u_1\frac{\partial u}{\partial y}\frac{1}{\sqrt{1-u_2\frac{\partial u}{\partial y}}},\ v = v_w,\ T = T_w \ \ at\ y = 0 \tag{4}$$

$$u \to 0, T \to T_\infty\ at\ y \to \infty \tag{5}$$

The similarity transformation variables that are employed in the concurrent problem are:

$$\eta = \sqrt{\frac{b}{v_f}}y,\ u = bxf'(\eta),\ v = \sqrt{v_f b}\,f(\eta), \theta(\eta) = \frac{T - T_\infty}{T_w - T_\infty} \tag{6}$$

By implementing the aforementioned similarity transformation variable, equations (2)-(3), subject to the boundary constraints (4) and (5), can be revamped into the following array coupled equations.

$$\begin{aligned} &-f'(\eta)^2 + f(\eta).f''(\eta) + \frac{\mu_{Thnf}}{\mu_f}.\frac{\rho_f}{\rho_{Thnf}}.f''(\eta) \\ &+ \frac{\rho_f}{\rho_{Thnf}}.2K.f''(\eta)^2 + \frac{(\beta_T)_{Thnf}}{(\beta_T)_f}.G_r.\theta(\eta) = 0 \end{aligned} \tag{7}$$

$$\begin{aligned} &f(\eta).\theta'(\eta) + \frac{K_{Thnf}}{K_f}.\frac{(\rho C_p)_f}{\rho(C_p)_{Thnf}}.\frac{1}{P_r}.\theta''(\eta) \\ &+ \frac{(\rho C_p)_f}{\rho(C_p)_{Thnf}}.Se^{-n\eta}.\theta(\eta) - \gamma_3 f'(\eta) = 0 \end{aligned} \tag{8}$$

The revamped boundary constraints are (Li et. al.[20])

$$f(0) = S_*,\ f'(0) = 1 + \gamma_1\frac{f''(0)}{\sqrt{1-\gamma_2 f''(0)}},\ \theta(0) = 1 \tag{9}$$

$$f'(\infty) \to 0, \quad \theta(\infty) \to 0 \tag{10}$$

Here,

$$K = \frac{\alpha_1 b}{\rho_f v_f},\ G_r = \frac{\beta_T(T_w - T_\infty)}{b^2 x},\ S = \frac{Q}{b(\rho C_p)_f},$$

$$\gamma_3 = \frac{\gamma x}{T_w - T_\infty},\ \gamma_1 = u_1 b\sqrt{\frac{b}{v_f}},\ \gamma_2 = u_2^* ab\sqrt{\frac{b}{v_f}},\ u_2(x) = \frac{a}{x}u_2^*$$

The authors are also curious to assess the consequences of the dimensionless physical parameters on the rate of stress proximate to the surface (Skin friction coefficient) and the rate of thermal transmission (Nusselt Number) near the surface.

$$Skin\ Friction\ Coefficient = Cf_x\sqrt{Re_x} = \frac{\mu_{Thnf}}{\mu_f}f''(0)$$

$$Nusselt\ Number = \frac{Nu_x}{\sqrt{Re_x}} = -\frac{K_{Thnf}}{K_f}\theta'(0)$$

Elucidation of Physical Variables Pertinent to Prevailing Ternary Hybrid Nanofluid (Abbas et. al.[23])

Density

$$\rho_{Nf} = (1 - \phi_{S1})\rho_f + \phi_{S1}\rho_{S1}$$
$$\rho_{Hnf} = (1 - \phi_{S2})\rho_{Nf} + \phi_{S2}\rho_{S2}$$
$$\rho_{Thnf} = (1 - \phi_{S3})\rho_{Hnf} + \phi_{S3}\rho_{S3}$$

Dynamic viscosity

$$\mu_{Thnf} = \mu_f(1 - \phi_{S1})^{-\frac{5}{2}}(1 - \phi_{s2})^{-\frac{5}{2}}(1 - \phi_{s3})^{-\frac{5}{2}}$$

Thermal conductivity

$$k_{Nf} = k_f\left\{\frac{k_{S1} + (m-1)k_f - (m-1)\phi_{S1}(k_f - k_{S1})}{k_{S1} + (m-1)k_f + \phi_{S1}(k_f - k_{S1})}\right\}$$
$$k_{Hnf} = k_{Nf}\left\{\frac{k_{S2} + (m-1)k_{Nf} - (m-1)\phi_{S2}(k_{Nf} - k_{S2})}{k_{S2} + (m-1)k_{Nf} + \phi_{S2}(k_{Nf} - k_{S2})}\right\}$$
$$k_{Thnf} = k_{Hnf}\left\{\frac{k_{S3} + (m-1)k_{Hnf} - (m-1)\phi_{S3}(k_{Hnf} - k_{S3})}{k_{S3} + (m-1)k_{Hnf} + \phi_{S3}(k_{Hnf} - k_{S3})}\right\}$$

Specific heat capacity

$$(\rho C_p)_{Nf} = (1 - \phi_{S1})(\rho C_p)_f + \phi_{S1}(\rho C_p)_{S1}$$
$$(\rho C_p)_{Hnf} = (1 - \phi_{S2})(\rho C_p)_{Nf} + \phi_{S2}(\rho C_p)_{S2}$$
$$(\rho C_p)_{Thnf} = (1 - \phi_{S3})(\rho C_p)_{Hnf} + \phi_{S3}(\rho C_p)_{S3}$$

Table 1. Thermo-physical characteristics of engine oil and the three different nanocomposites

Physical attribution	Engine oil	Ag	Graphene	Cu
$\rho\ (kgm^{-3})$	863	10500	2250	8933
$K\ (Wm^{-1}K^{-1})$	0.1404	429	2500	401
$\Sigma\ (sm^{-1})$	2.09×10^{-12}	6.3×10^7	1×10^7	59.6×10^6
$C_p\ (Jkg^{-1}K^{-1})$	2048	235	2100	385

MATERIALS AND METHODS

Initially, the non-dimensional higher-order ODEs reformulated into an equivalent first-order boundary value problem, incorporating the associated boundary conditions. Numerical solutions for the dimensionless ordinary differential equations are calculated using the widely used MATLAB bvp4c solver in conjunction with the shooting technique. The bvp4c solver exhibits exceptional proficiency in managing boundary value problems, delivering precise outcomes even for complex or unstable systems due to its refined mesh adaptation process. This function enhances computational efficiency by minimizing processing effort and maximizing the overall performance of numerical computation. In order to utilize the bvp4c solver effectively, an initial guess conforming to its spatial constraints is required. The bvp4c solver, with a convergence threshold set at 10^{-4}, proves to be the most suitable method for estimating the numerical solutions of such intricate non-dimensional ODEs, outperforming other techniques in terms of accuracy. The validation of the employed methodology is demonstrated in Table 2.

RESULT AND DISCUSSION

The furnished second grade ternary hybrid nanofluid flow under investigation is generated by a transverse stretching surface subject to Thomson and Troian slip velocity. Furthermore, the thermo-convection effect alongside the exponential heat source is incorporated into the thermal boundary layer equation to enhance the thermal gradient over the flow geometry. The entire set of coupled equations that represent the physical flow geometry is based on the Cross-Hamilton nanofluid model [23]. As the addition of silver, copper and graphene nanocomposite to the second-grade fluid escalates the thermo-physical characteristic of second grade fluid, that is why the whole study is analyzed with second grade ternary hybrid nanofluid.Table 1 reflects the thermo-physical characteristics of engine oil and the three different nanocomposites, and Table 2 delineates the infallibility of the current investigation, which is an analogy to the finding of Devi and Devi [25] and Wang [26]. The graphical representation of the velocity and thermal distribution curve for the variation in different non-dimensional factors are sketched keeping fixed, $S = 0.1$, $K = 0.10$, $\gamma_1 = 0.1$, $\gamma_2 = 0.1$, $\gamma_3 = 0.1$, $S_* = 0.1$, $n = 2$.

Table 2. Resemblance of -θ'(0) with the results procured by Devi and Devi [25] and Wang [26] [created by author]

Pr	Devi and Devi[25]	Wang[26]	Present study with $S, \gamma_3 = 0$
2.0	0.91135	0.9114	0.9114
7.0	1.89540	1.8954	1.8954
20.0	3.35390	3.3539	3.3539

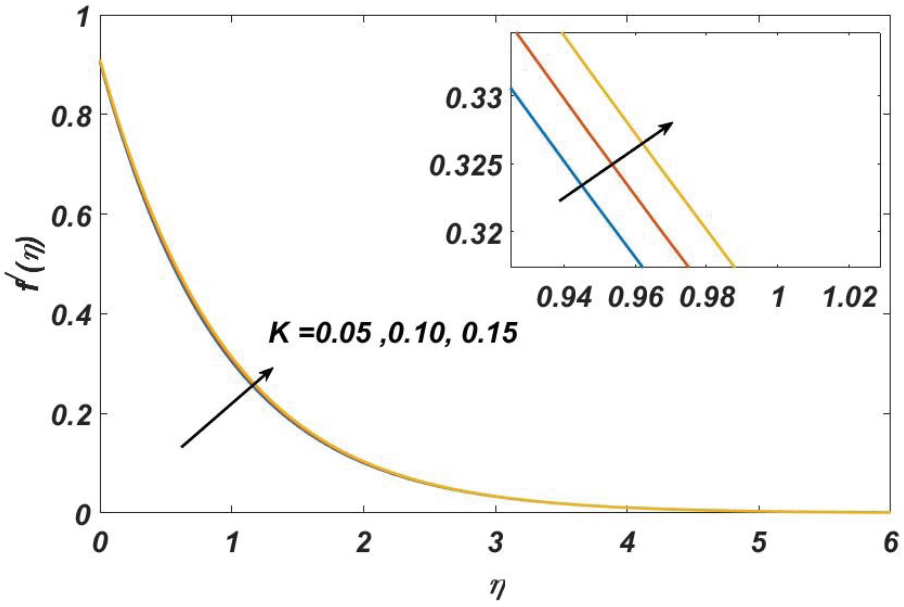

Figure 2. Impact of K on velocity distribution profile.

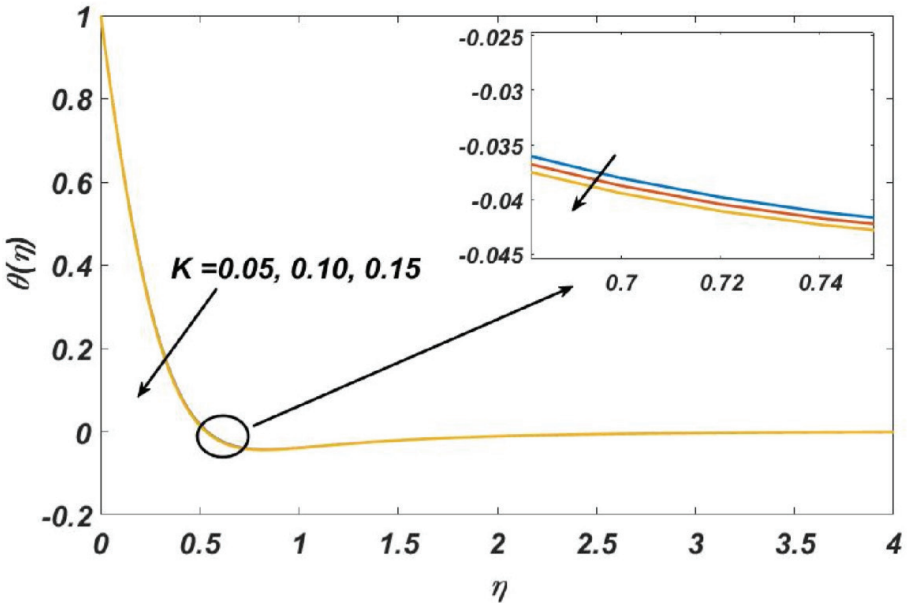

Figure 3. Impact of K on Thermal distribution profile.

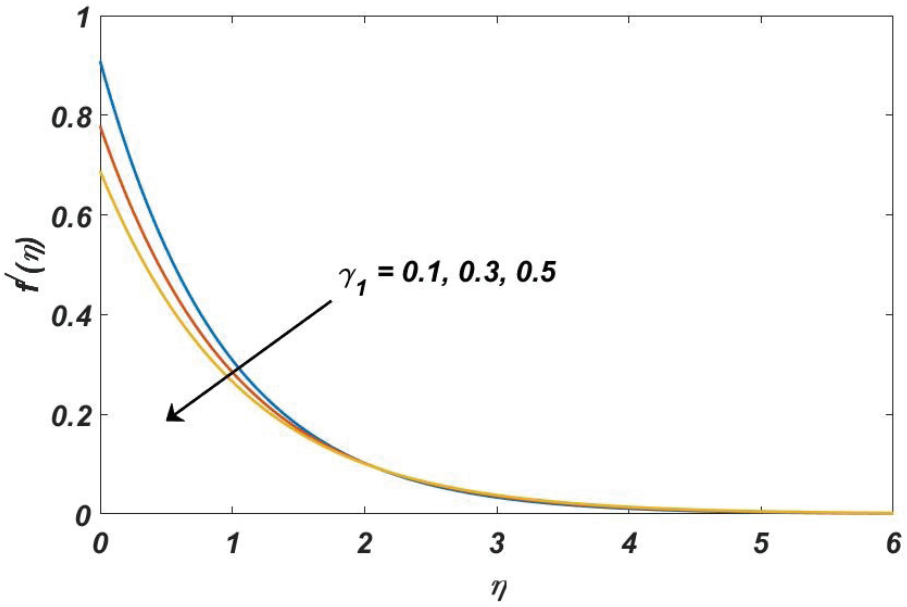

Figure 4. Impact of γ_1 on Velocity distribution profile.

In Figure 2 and Figure 3, the impact of the second-grade fluid factor on velocity and thermal distribution profile are portrayed. It has been observed that with the elevation in the numeric value of the second-grade fluid parameter, the flow profile looked to be an upsurge, while the thermal distribution profile exhibits a revert trajectory. Shah et al.[8] have obtained similar results over stretchable riga sheets for the velocity profile, opposite to the result proclaimed by Hosseinzadeh et. al. [7]. However, the impacts of the second-grade fluid parameter over the thermal profile have not been discussed by Shah et al. [8] and Hosseinzadeh et. al. [7]. Furthermore, as shown in Table 3, the reduction in the rate of tangential stress and the rate of thermal transmission at the vicinity of the stretch surface is perceived with the incremented values of the second-grade fluid parameter, K. The augmentation in K leads to the increment in elasticity, which in turn upsurges the fluid flow at the vicinity of the surface, as the fluid can stretch and flow more easily. Conversely, the increased elasticity efficiently limits the thermal transmission or energy exchange.

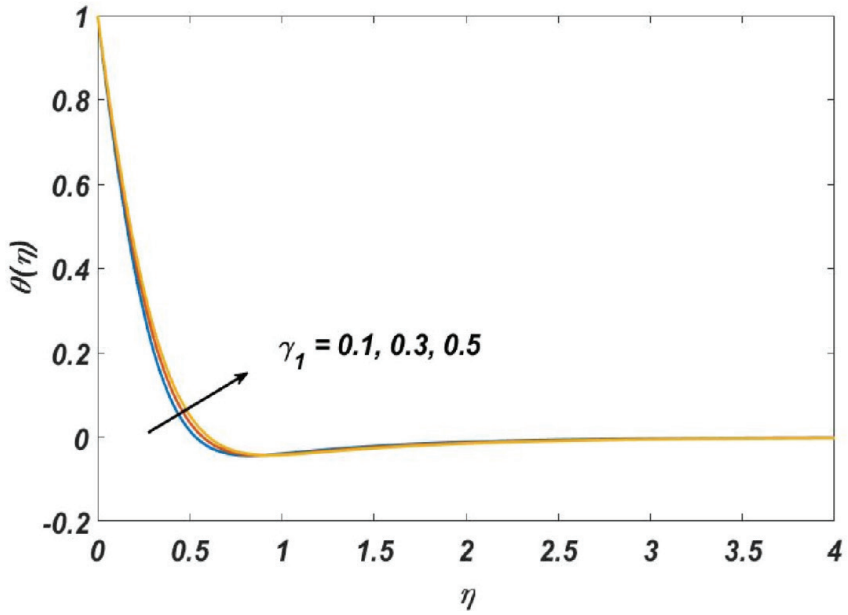

Figure 5. Impact of γ_1 on Thermal distribution profile.

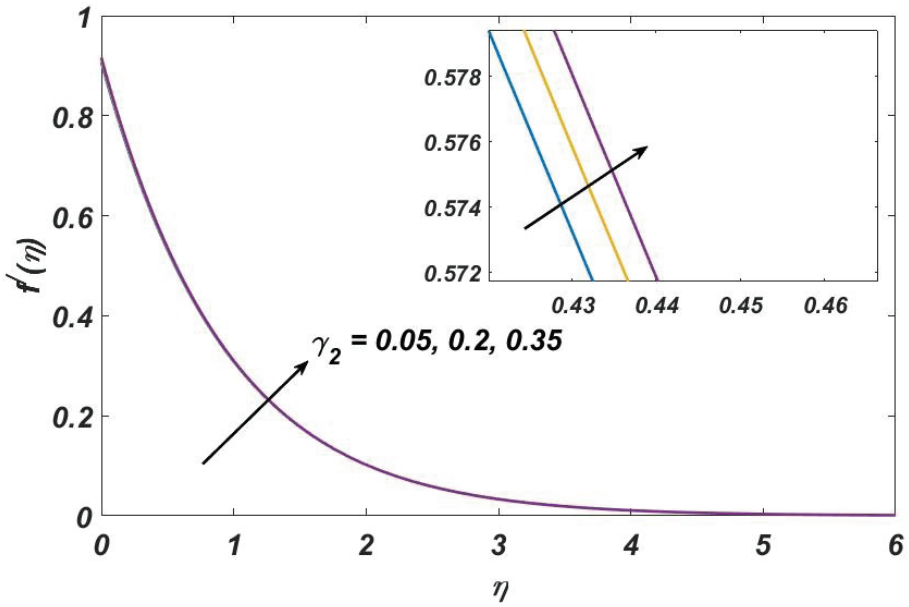

Figure 6. Impact of γ_2 on Velocity distribution profile.

The designated model is featured in a way where the boundary undergoes the consequences of Thomson slip velocity, which is depicted in Figure 4 and Figure 5. As shown in Figure 4, the velocity profile of second grade ternary hybrid Nanofluid promptly dropped with the numeric escalation of Thomson slip velocity, γ_1. Whereas the thermal distribution curve significantly arises for the numeric elevation of the slip factor γ_1 as shown in Figure 5. These results occur due to the fact that greater slip at the vicinity of the boundary reduces frictional drag. The reduced interaction with the boundary allows less momentum transfer, leading to a drop in velocity. Conversely, the thermal distribution increases because the reduced frictional drag indicates less energy is lost to resistance, allowing more energy to be retained in the fluid. The opposite pattern is noted in both velocity and thermal distribution profiles for rising factor γ_2 as shown in Figure 6 and Figure 7. When critical shear rate, γ_2 is uplifted, then the velocity curve appears to manifest an upward trend, whereas the thermal profile falls in a downward pattern. Over Newtonian fluid, similar results

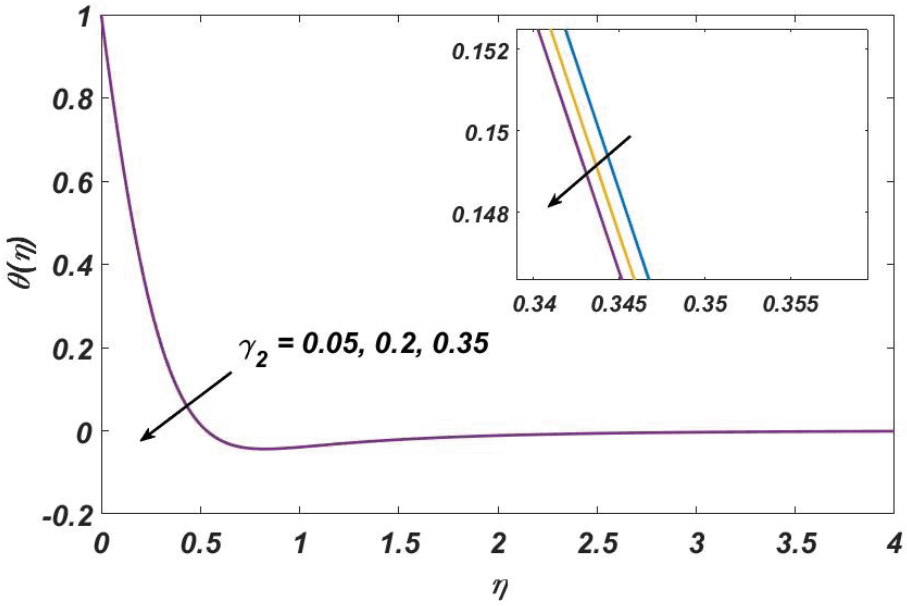

Figure 7. Impact of γ_2 on Thermal distribution profile.

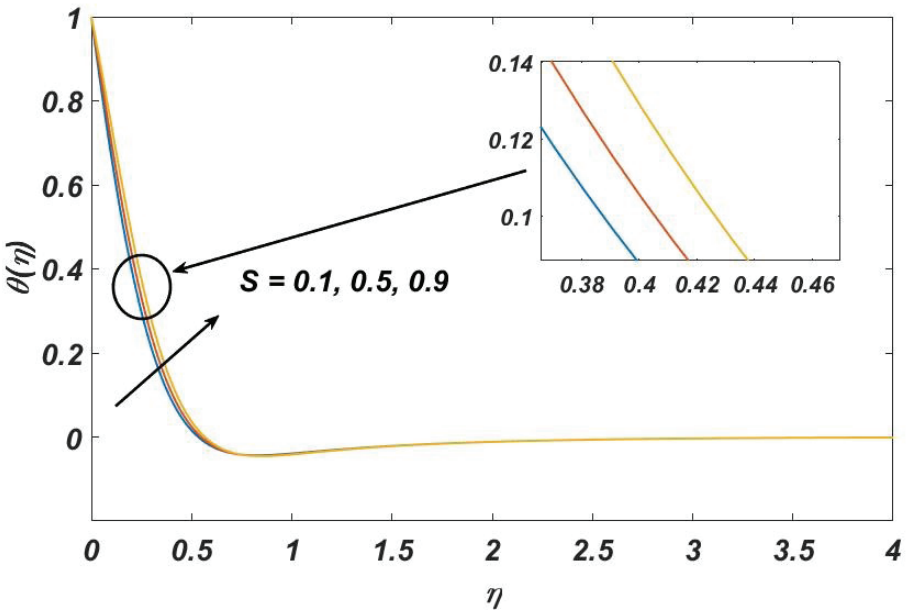

Figure 8. Impact of S on thermal distribution profile.

are obtained by Li et. al.[20] for the slip and critical shear factor.

Figure 8 and Figure 9 demonstrate the influences of exponential heat source, S and power law index, n over the thermal profile. The heat distribution profile looked to be upraised for both exponential heat source, S and power law index n, as shown in Figure 8 and Figure 9. It is because, with a greater thermal source factor and power law index (which intensify the heat source significantly), the nano-composites sop up that amount of thermal energy, which allows an extensive amount of diffusion of heat throughout the system. For non-exponential i.e. linear heat source, a similar pattern in the thermal profile is proclaimed by Li et al. [20] considering Newtonian hybrid nanofluid.

In Figure 10, 11, 12, the impacts of the thermo-convection parameter, γ_3 and suction velocity, S_* are portrayed respectively. Figure 10 illustrates a significant increase in the heat profile as the values of γ_3, indicative of thermo-convection or stratification, are raised. This enhancement is linked to the increased thermal gradients

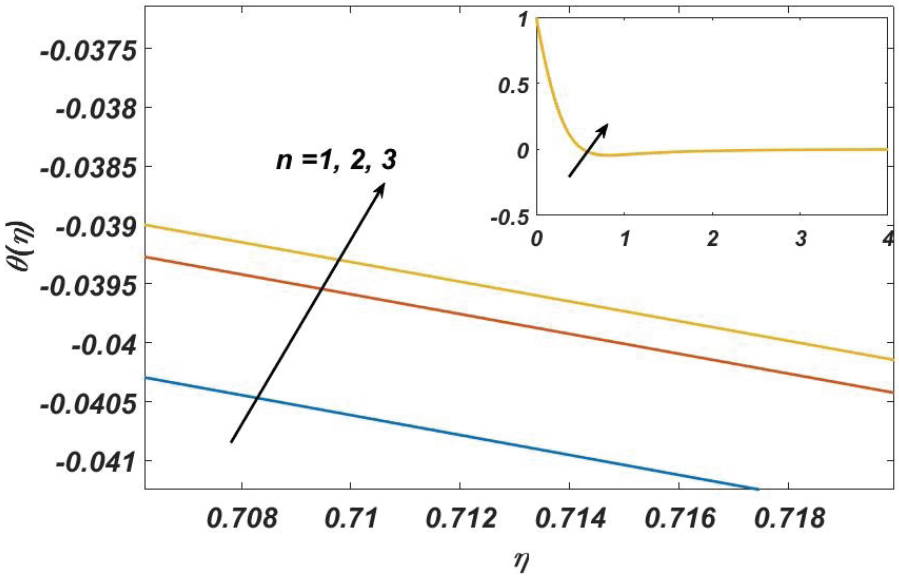

Figure 9. Impact of n on thermal distribution profile.

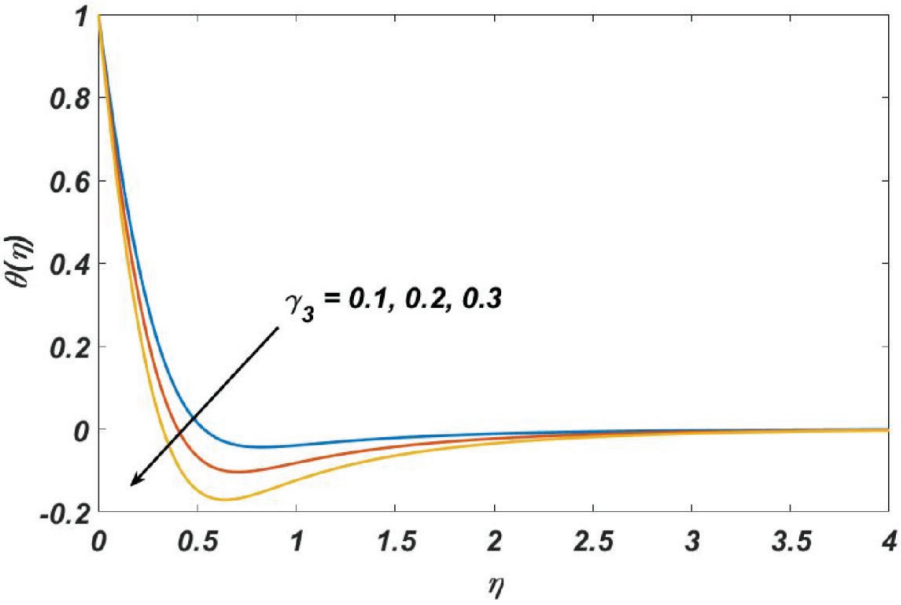

Figure 10. Impact of γ_3 on thermal distribution profile.

observed within the boundary layer of the second-grade ternary hybrid nanofluids. With a rise in the parameter value, the temperature difference between adjacent layers becomes more pronounced, promoting stronger and more effective interaction among the nanocomposite elements. Such intensified interaction enhances thermal convection, ensuring a more uniform spread of heat across the system. The increase in thermal diffusion arises from the intensified motion and interaction of the nanoparticles, which together enhance the overall efficiency of heat transmission. Consequently, the observed rise in temperature dispersion indicates higher thermal sensitivity and diffusion potential within the fluid, resulting from increased parameter magnitudes. Deka and Paul [24], found this result for unsteady Newtonian fluid past an infinite moving vertical cylinder.

Again, as portrayed in Figure 11, it has been significantly noted that the velocity profile shows a downward trajectory with a lofted suction velocity. The reason behind the downward trajectory of the velocity profile is the lower pressure created by the alofted suction velocity. Also, the increased suction velocity factor leads to a drop in the thermal distribution profile at the vicinity of the surface, and

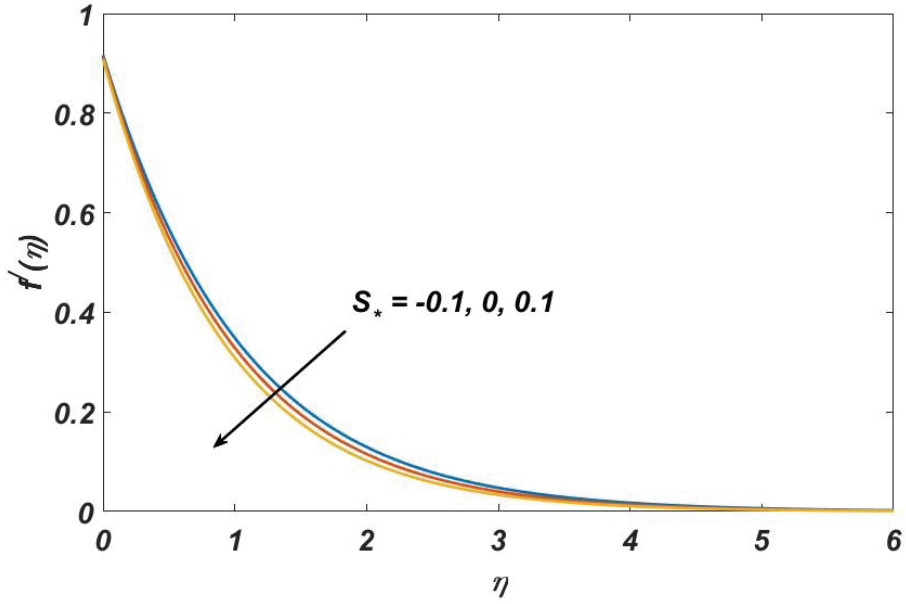

Figure 11. Impact of S_* on velocity distribution profile.

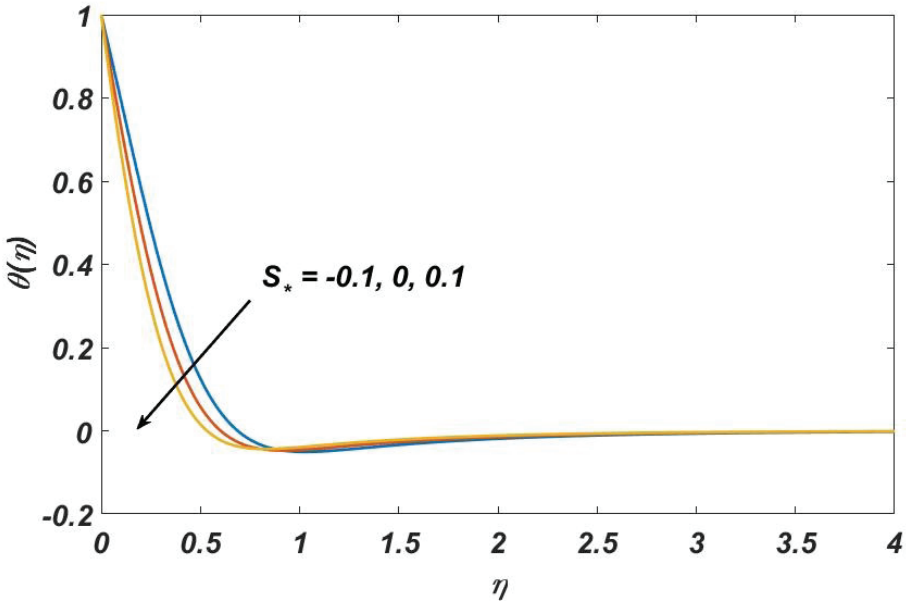

Figure 12. Impact of S_* on thermal distribution profile.

it is more significant due to thermal stratification or thermos-convection impact, as shown in Figure 12.

The impact of γ_1, γ_2, γ_3, K, S, S_* over the skin friction coefficient and Nusselt number are demonstrated in Table 3. It has been observed that the augmented value of the second grade fluid factor appears to decline the rate of shear stress proximate to the vertical surface. As K rises from 0.05 to 0.15, the reduced percentage in the rate of tangential stress at the vicinity is about 4.08%. This decline mainly results from the rise in viscosity linked to greater K values, which suppresses the fluid's reaction to shear stresses. Conversely, the Nusselt number shows an increase of about 0.52% as K changes from 0.05 to 0.15. This rise in the Nusselt number signifies improved convective heat exchange, resulting from changes in flow dynamics that facilitate a more uniform spread of thermal energy within the boundary layer. A similar pattern is also noted in the skin friction coefficient for the Thomson velocity slip parameter, γ_1, but the opposite is the pattern for critical shear rate, γ_2. Simultaneously, the Nusselt number shows a decline pattern in numeric with

Table 3. Demonstration of physical value of shear stress rate at vicinity, skin friction coefficient and thermo-efficiency rate at vicinity (Nusselt number) with varying dimensional parameter

S	K	γ_1	γ_2	γ_3	S^*	n	Skin friction coefficient	Nusselt number
0.1	0.10	0.1	0.1	0.1	0.1	2	-1.2048	4.6992
0.5							-1.2047	3.9555
0.9							-1.2047	3.1172
0.1	0.05	0.1	0.1	0.1	0.1	2	-1.2293	4.6867
	0.10						-1.2048	4.6992
	0.15						-1.1811	4.7115
0.1	0.10	0.1	0.1	0.1	0.1	2	-1.2048	4.6992
		0.3					-0.9653	4.4092
		0.5					-0.8094	4.1945
0.1	0.10	0.1	0.05	0.1	0.1	2	-0.9560	4.6954
			0.2				-1.2111	4.7064
			0.35				-1.2194	4.7158
0.1	0.10	0.1	0.1	0.1	0.1	2	-1.2048	4.6992
				0.2			-1.2048	5.4047
				0.3			-1.2048	6.1102
0.1	0.10	0.1	0.1	0.1	-0.1	2	-1.0922	2.5949
					0		-1.1471	3.5835
					0.1		-1.2048	4.6992
0.1	0.10	0.1	0.1	0.1	0.1	1	-1.2048	4.6839
						2	-1.2048	4.6992
						3	-1.2048	4.7146

rising values of S, γ_1. Moreover, it is noteworthy to mention that the heat transmission rate at the vicinity exhibits a prompt elevation in terms of values with the amplified second grade fluid factor (K), critical shear rate (γ_2), Thermo-convection parameter (γ_3), Suction parameter (S_*), Power law index (n).

CONCLUSION

The proposed model deals with the investigation of second grade ternary hybrid nanofluid flow subject to Thomson and Troian slip velocity featured by thermo-convection effect via stretching sheet. Graphene nanoparticles are used along with Ag and Cu due to their flexibility, high resistance, and high thermal conductivity. The following noteworthy discoveries have been made from the aforementioned investigation.

- The Velocity distribution profile raises for the higher value of the second-grade fluid parameter and critical shear rate. Higher second-grade fluid parameter typically corresponds to greater non-Newtonian effects, which can enhance velocity gradients in the boundary layer. Similarly, a greater critical shear rate implies that the fluid can sustain larger shear stresses without significant changes in flow characteristics.
- The velocity distribution profile also diminishes for higher values of Thomson and troian slip velocity and Suction parameter. Increased slip velocity at the boundary reduces the no-slip condition, allowing the fluid to slip more freely and thereby reducing the velocity gradients near the boundary. Also, increased suction draws fluid away from the surface, which diminishes the velocity distribution near the surface.
- The skin friction coefficient is boosted with a critical shear rate and suction parameter, while the skin friction coefficient dropped for higher values of non-dimensional heat source parameter, second-grade fluid parameter and Thomson and Troian slip velocity.
- The thermal distribution profile upsurges for bigger Thomson and Troian slip velocity, non-dimensional heat source parameter and power law index but reduces with a rise of second grade fluid parameter, critical shear rate, thermo-convection parameter and suction parameter. A higher Thomson and Troin slip velocity enhances thermal convection by reducing thermal boundary layers. Increased heat source represents a greater heat generation rate within the system, thus elevating the temperature distribution. An increased second-grade fluid coefficient suggests more dominant non-Newtonian characteristics, which may reduce the rate of heat transfer. Increased

critical shear rate signifies that the fluid's response to shear stresses is more constrained, affecting the thermal profile. A stronger thermo-convective effects that may alter heat transfer dynamics, and the increased suction suction velocity extracts heat from the surface, leading to lower thermal profiles.

- The Nusselt number augmented with elevated values of second grade fluid parameter, critical shear rate, thermo-convection parameter, suction parameter and power law index, conversely diminished with increasing values of non-dimensional heat source parameter and Thomson and Troian slip velocity.

The proposed framework holds broad potential in the field of advanced heat management, especially in improving cooling performance for electronic components, thermal exchangers, and other high-efficiency systems. Additionally, it delivers meaningful understanding for refining production techniques across sectors such as polymer fabrication and thin-film coating. Additionally, the model›s analysis of thermo-convection, buoyancy effects, and exponentially varying heat sources is crucial for improving cooling performance in aerospace and automotive systems and optimizing renewable energy technologies such as solar thermal collectors.

We can further extend this investigation to diverse geometrical configurations such as conical disks, rotating disks or spheres, concentric cylindrical channels, etc., considering the same or other constraints and factors, as it can broaden the applicability of the findings. This research provides a solid foundation for continued exploration of nanofluid dynamics and thermal transport processes. Researchers can build on the aforementioned findings to explore new material combinations and refine theoretical models in fluid dynamics and thermal management.

NOMENCLATURE

u_w	The surface velocity at vicinity (m/s)
u, v	Velocity along horizontal and vertical direction respectively (m/s)
g	Gravitational acceleration (m/s^2)
Q,S	Dimensionless ($JK^{-1}\ m^{-3}\ s^{-1}$) and non-dimensionless heat source factor
n	Power Law Index
v_w	Suction velocity (m/s)
K	Second grade fluid parameter
b	Rate of stretching (s^{-1})
T_w	Temperature at the vicinity of the wall (K)
T_∞	Temperature at the ambient (K)
$S_\star$	Suction parameter
Pr	Prandtl number
Gr	Grashof number
$(C_p)_f$, $(C_p)_{Nf}$	Specific heat capacity of base fluid (Engine Oil), Nanofluid ($J\ Kg^{-1}\ K^{-1}$)
$(C_p)_{Hnf}$, $(C_p)_{Thnf}$	Specific heat capacity of hybrid Nanofluid, Ternary hybrid Nanofluid ($J\ Kg^{-1}\ K^{-1}$)

Greek symbols

α_1	Second grade material constant
β_T	Thermal expansion coefficient (K^{-1})
γ_1	Thomson and Troian slip velocity
γ_2	Critical Shear rate
γ_3	Dimensionless Thermo-convection parameter
ρ_f	The density of the base fluid (Engine Oil) (kgm^{-3})
ρ_{Nf}	The density of the Nanofluid (kgm^{-3})
ρ_{Hnf}	Density of the Hybrid Nanofluid (kgm^{-3})
ρ_{Thnf}	The density of the Ternary Hybrid Nanofluid (kgm^{-3})

Subscripts

S1, S2, S3	Ag, Cu and Graphene nanoparticles
f	Base fluid (Engine Oil)
Nf	Nanofluid
Hnf	Hybrid Nanofluid
Thnf	Ternary Hybrid Nanofluid

AUTHORSHIP CONTRIBUTIONS

Authors equally contributed to this work.

DATA AVAILABILITY STATEMENT

The authors confirm that the data that supports the findings of this study are available within the article.

CONFLICTS OF INTEREST

The authors declare no conflict of interest.

FUNDING

Not Applicable

REFERENCES

[1] Roy NC, Pop I. Flow and heat transfer of a second-grade hybrid nanofluid over a permeable stretching/shrinking sheet. Eur Phys J Plus 2020;135:768. [CrossRef]

[2] Nadeem M, Siddique I, Awrejcewicz J, Bilal M. Numerical analysis of a second-grade fuzzy hybrid nanofluid flow and heat transfer over a permeable stretching/shrinking sheet. Sci Rep 2022;12:1631. [CrossRef]

[3] Jawad M, Saeed A, Tassaddiq A, Khan A, Gul T, Kumam P, Shah Z. Insight into the dynamics of second grade hybrid radiative nanofluid flow within the boundary layer subject to Lorentz force. Sci Rep 2021;11:4894. [CrossRef]

[4] Roy NC, Ghosh A. Magnetohydrodynamic natural convection of second-grade hybrid nanofluid on variable heat flux surface. AIP Adv 2022;12: 035243. [CrossRef]

[5] Sakthi I, Das R, Reddy PBA. Entropy generation on MHD flow of second-grade hybrid nanofluid flow over a converging/diverging channel: An application in hyperthermia therapeutic aspects. Eur Phys J Spec Top 2023:;233:1233–1249. [CrossRef]
[6] Zulqarnain RM, Nadeem M, Siddique I, Mansha A, Ghallab AS, Samar M. Impacts of entropy generation in second-grade fuzzy hybrid nanofluids on exponentially permeable stretching/shrinking surface. Sci Rep 2023;13:22132. [CrossRef]
[7] Hosseinzadeh K, Mardani MR, Paikar M, Hasibi A, Tavangar T, Nimafar M, Shafii MB. Investigation of second grade viscoelastic non-Newtonian nanofluid flow on the curve stretching surface in presence of MHD. Results Eng 2023;17:100838. [CrossRef]
[8] Shah F, Hayat T, Momani S. Non-similar analysis of the Cattaneo–Christov model in MHD second-grade nanofluid flow with Soret and Dufour effects. Alex Eng J 2023;70:25–35. [CrossRef]
[9] Abbas N, Ali M, Shatanawi W. Chemical reactive second-grade nanofluid flow past an exponential curved stretching surface: Numerically. Int J Mod Phys B 2023;38:2450026. [CrossRef]
[10] Zaman T, Shah Z, Rooman M, Khan W, Garalleh HA. Computation analysis of unsteady second grade biomagnetic micropolar blood-based nanofluid flow with motile gyrotactic microorganisms. Int J Model Simul 2024:1–18. [CrossRef]
[11] Gangadhar K, Sujana Sree T, Thumma T. Impact of Arrhenius energy and irregular heat absorption on generalized second-grade fluid MHD flow over nonlinear elongating surface with thermal radiation and Cattaneo–Christov heat flux theory. Mod Phys Lett B 2024;38:2450077. [CrossRef]
[12] Farooq U, Irfan M, Khalid S, Jan A, Hussain M. Computational convection analysis of second-grade MHD nanofluid flow through porous medium across a stretching surface. Z Angew Math Mech 2024:e202300401. [CrossRef]
[13] Rath C, Nayak A. MHD second-grade nanofluid slip flow over a stretching sheet subject to activation energy, thermophoresis, and Brownian effects. Phys Scr 2024;99:035228. [CrossRef]
[14] Khan MN, Khan AA, Alqahtani MA, Wang Z, Hejazi HA, AzZo'bi EA. Chemically reactive aspects of stagnation-point boundary layer flow of second-grade nanofluid over an exponentially stretching surface. Numer Heat Transf B Fundam 2025;86:1622–1638.
[15] Kezzar M, Talbi N, Dinarvand S, Das S, Sari MR, Nasr S, Akhlaghi Mozaffar A. Velocity slip and temperature jump effects on entropy generation of MHD second-grade hybrid nanofluid in Jeffery–Hamel flow. Int J Numer Methods Heat Fluid Flow 2024;34:3637–3658. [CrossRef]
[16] Reza-E-Rabbi S, Ali MY, Ahmmed SF. Nonlinear radiative second-grade nanofluid with sinusoidal magnetic force and Arrhenius activation energy: A computational exploration. Alex Eng J 2024;104:66–84. [CrossRef]
[17] Haq SU, Ali F. Analysis of Newtonian heating in fractional hybrid nanofluid with the influence of transverse magnetic field. Int J Heat Fluid Flow 2024;106:109293. [CrossRef]
[18] Ahmed MF, Yasmin H, Ali F, Raizah Z, Lone SA, Saeed A. MHD flow of second-grade fluid containing nanoparticles having gyrotactic microorganisms across heated convective sheet. Z Angew Math Mech 2024;104:e202300950. [CrossRef]
[19] Akaje TW, Olajuwon BI, Musiliu Tayo RAJI. Computational analysis of the heat and mass transfer in a Casson nanofluid with a variable inclined magnetic field. Sigma 2023;41:512–523. [CrossRef]
[20] Li S, Puneeth V, Saeed AM, Singhal A, Al-Yarimi FA, Khan MI, et al. Analysis of the Thomson and Troian velocity slip for the flow of ternary nanofluid past a stretching sheet. Sci Rep 2023;13:2340. [CrossRef]
[21] El Hattab M, Boumhaout M, Oukach S. MHD natural convection in a square enclosure using carbon nanotube–water nanofluid with two isothermal fins. Sigma J Eng Nat Sci 2024;42:1075–1087. [CrossRef]
[22] Nath JM, Paul A, Das TK. Heat transfer characteristics of magnetohydrodynamic Casson stratified hybrid nanofluid flow past a porous stretching cylinder. J Therm Eng 2021;10:1137–1148. [CrossRef]
[23] Abbas M, Khan N, Hashmi MS, Alotaibi H, Khan HA, Rezapour S, et al. Importance of thermophoretic particles deposition in ternary hybrid nanofluid with local thermal non-equilibrium conditions: Hamilton–Crosser and Yamada–Ota models. Case Stud Therm Eng 2024;56:104229. [CrossRef]
[24] Deka RK, Paul A. Convectively driven flow past an infinite moving vertical cylinder with thermal and mass stratification. Pramana 2013;81:641–665. [CrossRef]
[25] Devi SU, Devi SA. Heat transfer enhancement of Cu–Al_2O_3/water hybrid nanofluid flow over a stretching sheet. J Niger Math Soc 2017;36:419–433.
[26] Wang CY. Free convection on a vertical stretching surface. Z Angew Math Mech 1989;69:418–420. [CrossRef]
[27] Zulqarnain RM, Nadeem M, Siddique I, Samar M, Khan I, Mohamed A. Numerical study of second-grade fuzzy hybrid nanofluid flow over the exponentially permeable stretching/shrinking surface. Front Phys 2023;11:1301453. [CrossRef]
[28] Siddique I, Khan Y, Nadeem M, Awrejcewicz J, Bilal M. Significance of heat transfer for second-grade fuzzy hybrid nanofluid flow over a stretching/shrinking Riga wedge. AIMS Math 2023;8:295–316. [CrossRef]
[29] Ali Q, Riaz S, Memon IQ, Chandio IA, Amir M, Sarris IE, Abro KA. Investigation of magnetized convection for second-grade nanofluids via Prabhakar differentiation. Nonlinear Eng 2023;12:20220286. [CrossRef]